วิศวกรรมสาร มข. ปีที่ 37 ฉบับที่ 1 (55 - 63) มกราคม - มีนาคม 2553 บทความวิจัย
KKU Engineering Journal Vol.37 No.1 (55 - 63) January - February 2010

Prediction of Head Stack Assembly Gram Load Using Finite Element Analysis

Khemakorn Chaloemsri[1)] and Sujin Bureerat [*2)]

Abstract

This paper presents a finite element model for simulating a swaging process of a hard disk drive (HDD) head stack assembly (HSA). The swaging process is a material processing technique using swage balls to connect a suspension system to an E-block which becomes the so-called head stack assembly. The finite element (FE) model is three-dimensional using an explicit dynamics simulation with solid Lagrangian elements. In this paper, the base plate and arm tip deformations due to ball swaging and the impact of the head stack gram load value are evaluated. The simulation results are compared to those obtained from experimentation. It was found that the results from FE analysis are well-corresponding to the experiment results.

Keywords: Finite element analysis, Swaging process, Hard disk drive, Contact analysis, Head stack Assembly.

[1)] Post Graduated Student, Department of Mechanical Engineering, Faculty of Engineering, Khon Kaen University, Thailand, 40002

[*2)] Association Professor, Department of Mechanical Engineering, Faculty of Engineering, Khon Kaen University, Thailand, 40002, Corresponding Author, E-mail: sujbur@kku.ac.th

1. Introduction

In the HDD manufacturing process, ball swaging is one of the most important manufacturing processes which joins the head gimbal assembly (HGA) base plates together with an actuator arm resulting in a new part called the head stack assembly (HSA). The HGA base plate is a thin sheet component, which includes the boss tower, as illustrated in Figure 1. The boss tower is sized to fit within an opening in the actuator arm to which the HGA base plates are to be mounted. During the swaging process, the ball is driven to pass through the boss tower into the inner surface of the opening in the actuator arm and clamped by swage keys. The baseplate and attached suspension are thereby securely fastened to the actuator arm. To hold the HGA in place, the interface between the base plate and actuator arm must develop a suitable minimum retention torque value. A specific value of retention torque at the joint is required to withstand the vibrations of the actuator arm that are induced by the high-speed unstable airflow in the drive. A view of the process of assembly by swaging is shown in Figure 2.

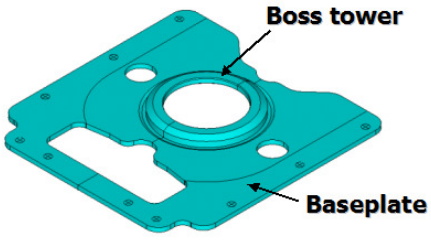

Fig.1 *Components of a baseplate*

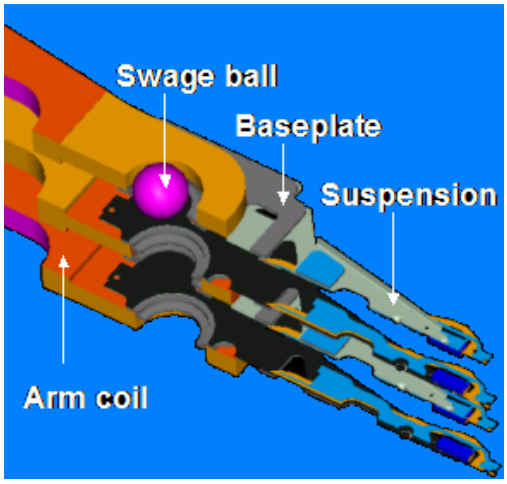

Fig. 2 *The assembly for swaging process*

Unfortunately, this swaging process can result in an undesirable plastic deformation of the HGA base plate and actuator arm. These deformations can cause a change, known as gram load change, in the desired spring characteristics of the suspension on the actuator arm, from its nominal value, and also a change of the desired retention torque. Since gram load and retention torque are the critical parameters affecting the slider flight height and op-shock performance of hard disk drives, an investigation of the base plate and arm deformation, the gram load as well as retention torque change, which are induced by the swaging process, is of general interest.

The work by Wadhwa (S.K. Wadhwa, 1996) is one of the early numerical analyses of the ball swaging process using an axis-symmetric model of the in-plane deformation. Aoki and Aruga (Aoki and Aruga, 2007) performed an elasto-plastic large deformation analysis based on a symmetrical model for ball swaging and clarified that the baseplate is influenced by the arm deformation due to the asymmetric stress. Kamnerdtong et al. (Kamnerdtong, S.Chutima and K.Ekintumas, 2005) numerically verified the effects of the swaging

process parameters, including the size, velocity and shooting direction of the swage ball, by using an axis-symmetric finite element analysis (FEA). Some of the recommendations which were given regarding the torque resistance show it was dominated by contact pressure during the swaging process and an undesirable higher stress intensity in the necking zone of the baseplate resulted in greater deformation of the arm. Jian Yang et al. (Jian Yang, Chen-Chi Lin and Shahab Tabrizi, 2007) performed a comprehensive three-dimensional finite element analysis of ball swaging process with 2 swage keys and 2 - swage balls for both inner and outer arms with attached base plate(s). The changes of the gram load on the sliders were estimated from the nominal gram load value and the gram load deviation due to the deformation of the base plate and arm. The estimated gram load values also correlate well with the average test data. Further work investigating a swaging process using computational contact mechanics can be found in (Jongpradist, et al., 2009; J.R. Cho, et al., 2005; DreanM, 1998; Li RONG, Zuo-ren NIE and Tie-yong ZUO, 2006; Zhi-Hua Zhong, 1993) However, review of the literature shows that an investigation of swaging with bi-directional swaging by using 3-Balls induced gram load and retention torque change is still open and challenging.

The aim of this work is to determine the effects resulting from a bi-directional swaging process by initiating a comprehensive, three-dimensional finite element analysis model (FEA). In the present work, the swaging process is studied by performing an explicit dynamic finite element analysis (FEA) using the commercial program ANSYS/LS-Dyna. Both one-sided and two-sided top arm in the assembly are opted as a prototype to be studied. The 3 - Balls swaging process is considered where the ball diameters are 0.0780" (1st pass), 0.0810" (2nd pass), 0.0820" (3rd pass flip), with their velocities maintained as constant at 0.7in/s in the top-to-bottom direction.

2. Finite Element Modeling

The use of finite element analysis for material processing techniques, particularly for those involving contact mechanics, has been studied for many years (Zhong, 1993). A contact system of multiple deformable bodies can be thought of as a system being in an equilibrium state such that contact constraints (no penetration between bodies) are imposed on the surfaces of the bodies touching each other. The equation of motion of a body occupying a space domain Ω can be written as (Zhong, 1993)

$$\frac{\partial \sigma_{ji}(\mathbf{x},t)}{\partial x_j} + b_i(\mathbf{x},t) = \rho a_i(\mathbf{x},t) \quad \text{for } i = 1, \ldots, 3 \text{ and } j = 1, \ldots, 3 \tag{1}$$

where **x** is a point on Ω, σ_{ji} is a Cauchy stress component, **b** is a body force vector, ρ is material density, and **a** is an acceleration vector. The boundary of the body Ω can be defined as Γ, and it is divided into three distinct parts as

$$\Gamma = \Gamma_d \cup \Gamma_f \cup \Gamma_c \tag{2}$$

Where Γ_d is the boundary part having prescribed displacements, Γ_f is the boundary part that has prescribed forces and Γ_c is the boundary part contacting to other bodies. The prescribed boundary conditions can be written as

$$u_i(\mathbf{x},t) = \bar{u}_i(\mathbf{x},t); \mathbf{x} \in \Gamma_d$$
$$\sigma_{ij}(\mathbf{x},t)N_j = \bar{q}_i(\mathbf{x},t); \mathbf{x} \in \Gamma_f \quad (3)$$

Where $\bar{u}_i$ and $\bar{q}_i$ are prescribed displacement and boundary traction components respectively. N_j is the component of an outward normal vector at **x** on Γ_f. The initial conditions for displacement (**u**) and velocity (**v**) are also required as:

$$\mathbf{u}(\mathbf{x},0) = \bar{\mathbf{u}}(\mathbf{x}); \mathbf{x} \in \Omega$$
$$\mathbf{v}(\mathbf{x},0) = \bar{\mathbf{v}}(\mathbf{x}); \mathbf{x} \in \Omega \quad (4)$$

Where $\bar{\mathbf{u}}$ and $\bar{\mathbf{v}}$ are the prescribed displacement and velocity, respectively. The contact constraints are assigned in such a way that the contact stress should be negative (or compressive) whereas there is no penetration between bodies. The contact constraints on Γ_f can be expressed as:

$$g(\mathbf{x},t) = g(\mathbf{x},0) - \mathbf{u}(\mathbf{x},t)\cdot\mathbf{N} \geq 0; \mathbf{x} \in \Gamma_c$$
$$\bar{\mathbf{q}}_c(x,t)\cdot\mathbf{N} \leq 0; \mathbf{x} \in \Gamma_c \quad (5)$$

Where *g* is the gap between contact surfaces, and $\mathbf{q}_c$ is the contact traction.

By means of finite element analysis, the mathematical model (1) to (5) can be simplified to the matrix form of the system of second order differential equations. Using an explicit time integration technique can then solve the system of differential equations. Several numerical schemes deal with the contact constraints (5), part to part contact with a proper coefficient of friction. These methods have been implemented on numerous real world contact problems successfully.

2. Swaging Process Modeling

The finite element simulation of the ball swaging process was performed with the commercial software package. A three-dimensional (3-D) view and a cross-sectional view of the finite element (FE) model used for the swaging process of actuator arms are shown in Figure 3.

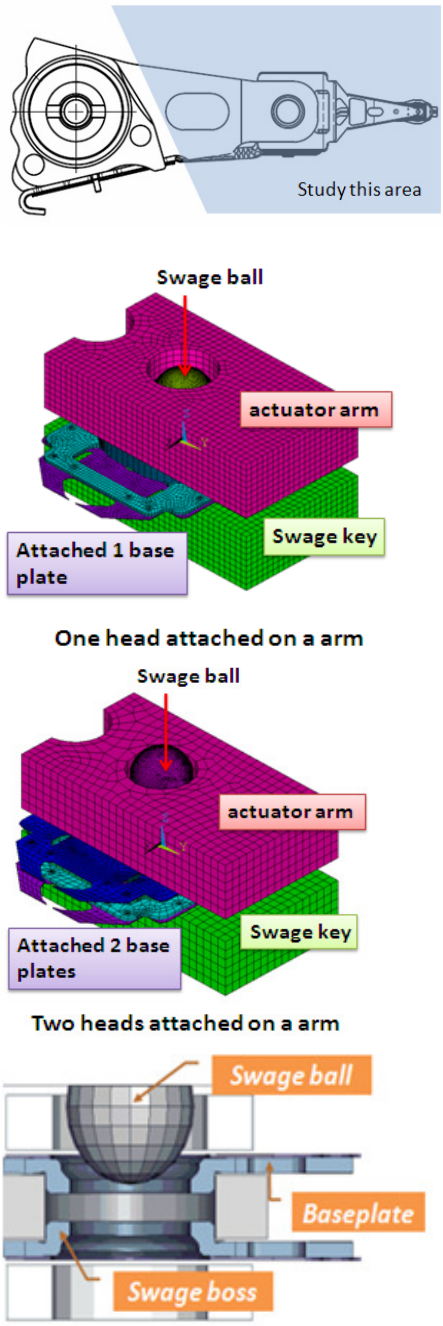

Fig. 3 *3D view of the finite element model used for swaging simulation of an actuator arm and attached base plates*

In this simulation, we performed a nonlinear explicit dynamics analysis. If the stress is in the elastic deformation region, the relationship between stress and strain is linear. After the stress reaches the yield point, the relationship becomes nonlinear and the swaged part of the base plate undergoes plastic deformation. Nonlinear material properties should be considered. Geometric non-linearity is also considered in this analysis because the base plate undergoes large deformation at the swaged part, as shown in Figure 4.

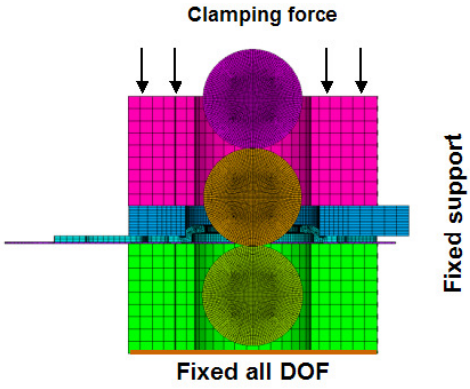

Fig. 4 *Boundary conditions of the FE model cross section*

The model includes an actuator arm tip, two base plates with part of hinges, two swage keys, and three swage balls. The base plate is attached to the one-side and two-side arms as shown in Figure 5. The base plate shape and profile illustrated in Figure 6 is chosen to investigate. To incorporate the elastic-plastic behavior of the actuator arm and base plates, these parts are modeled as bilinear isotropic material for baseplate and hinge, and bilinear kinematics hardening materials for an aluminum actuator arm.

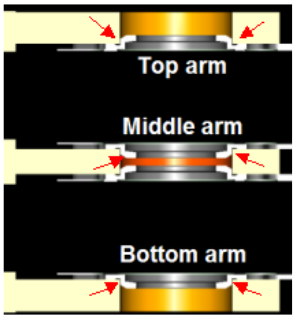

Fig.5 *model for one-sided and two-sided swaging*

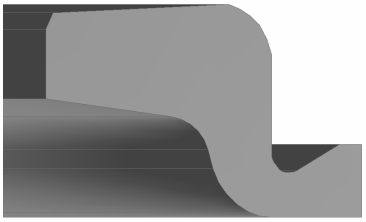

Fig. 6 *Base plate model*

3.1 Boundary Conditions and Contact Surfaces

During the swaging process, the constant clamping force at the outer parts during swaging is 65 psi and the arms are separated from each other by the use of spacer keys. In the FE model, the clamping pressure is applied as forces acting at a reference point on a prepared area. For simplicity, the swage keys, which are employed to simulate the clamping boundary at the arm contact condition, are modeled as rigid bodies while the other components including the actuator arm tip, the base plates and the hinges are deformable parts. The simulation uses the same load curve for ball speed for each head and the swage ball is constrained to move in the *Z* direction only.

The boss of the base plate is plastically deformed and joined to the arm. The contact surface between the ball and swaging boss, between the base plate and the arm, and the one between the swaging boss and the clamp are taken into account in analyzing the contact pressure. The friction coefficients for each contact surface are

separated into 2 groups as contact surface of assembly and part-to-part.

3.2 Material Properties

The base plate, hinge and the suspension are made of stainless steel while the arm is made of aluminum. The swaging ball is made of stainless steel with a hardened coating. Thus, the ball is simulated as a rigid body. The material models defined in the analysis are bilinear isotropic material and bi-linear kinematics hardening. The properties of the materials used in the simulation are listed in Table 1.

Table 1 *Material property for finite element analysis*

Material Properties	Type of Material	
	Stainless steel	Aluminum
Elastic modulus, E (MPa)	190,000	71,016
Yield stress, Y (MPa)	206	275
Poisson ratio	0.32	0.33
Mass density (kg/m^3)	7889	2700

*** Some components use bilinear isotropic material

All the elements used in the analysis are eight-nodes brick elements. To reduce the computing time, the model consists of both rigid bodies and deformable bodies. The actuator arm hole and the base plate boss tower are prepared such that finer meshes are only required in the vicinity of the contact areas and the elements are coarser in the areas farther away. Meshing of the structure is portrayed in Figure 7.

Fig. 7 *Meshing of the cross section finite element model*

3.3 Loading Conditions and Analysis

The analysis is performed using the following steps. Firstly, a compressive clamping force is applied to the prepared area on the top of the spacer key. Next, the swaging ball is driven through. After the swage ball has passed through, the clamping force is then released. After that, the upper and lower keys are ejected to allow final deformation of the assembly. The results for tip height and tip pitch are evaluated. The deformation is measured and evaluated at each node. The node location and section for measurement are determined.

4. Validation of the Finite Element Model

The base plate and arm tip deformation results from FEA simulations for inner and outer arms are evaluated from the displacement values measured from selected nodes compared to the reference plane. The measurement section is shown in Figure 8. Then, the results are calculated and reported as the tip height and the tip pitch deviations from nominal value, which is multiplied by a correction factor. The illustration of baseplate deformation from the FE swaging process is given in Fig. 9.

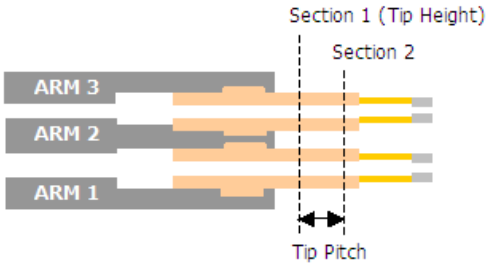

Fig. 8 *Measurement point for arm Tip Height and Tip pitch*

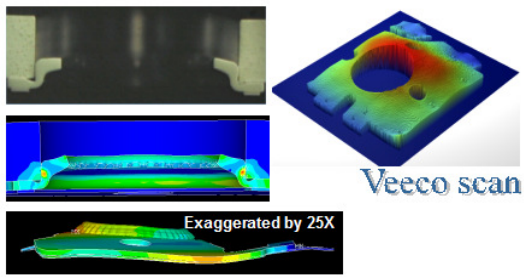

(a)

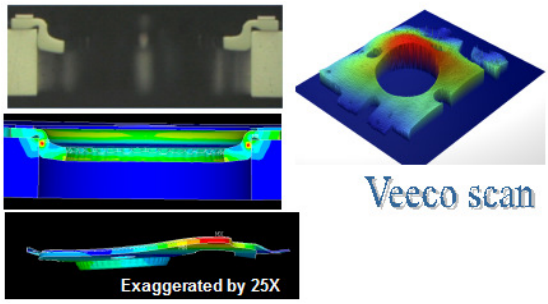

(b)

Fig. 9 *FEA results of baseplate deformation from swaging process (exaggerated by 25 times) for (a) DN facing head and (b) UP facing head*

Table 2 shows the comparison of the tip height and tip pitch obtained from FE simulation and experiment. It can be seen that the computational results acceptably correspond to those from experimentation. Thus, the result from this finite element model will be used for gram load calculation.

Table 2 *Simulation and experimental results*

Parameters		Tip Height (inch)		Tip Pitch (degree)	
		FEA result	Actual data	FEA result	Actual data
Head #0	Outer arm	0.00153	0.00123	-0.737	-0.535
Head #1	Inner arm	-0.00146	-0.00192	-0.469	-0.320
Head #2	Inner arm	-0.00050	-0.00060	-0.233	-0.216
Head #3	Outer arm	0.00064	0.00070	0.581	0.347

4.1 Gram Load Calculation

The definition of gram load is the reaction force at the loading point when the suspension assembly is elevated to an offset height. The gram load will be calculated from a specific equation at the effective slider z-height at loaded state. The suspension assembly model is created for simulating gram load on sliders by using tip height and the tip pitch input from the previous FE simulation. A three-dimension (3-D) view of the finite element (FE) model used for suspension is shown in Figure 10.

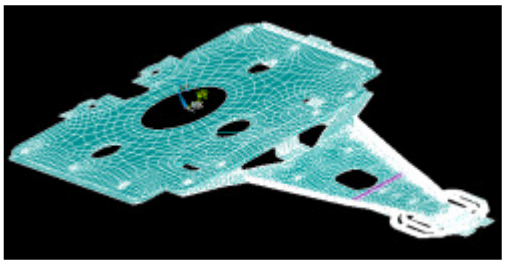

Fig. 10 *3-D view of the finite element model used for gramload simulation of suspension*

Table 3 shows the comparison of gram load obtained from FE simulation and from experiment. For all simulation cases, the simulation results somewhat correlate with the experiment. However, there are some errors that require further investigation. These differences could be from some other effects being ignored in the present analysis, such as the uncertainties of swage key shape and swage boss profile which are different from actual parts. Structural imperfection also plays a crucial role in this comparison.

Table 3 *Gramload Simulation and experimental results*

Parameter		Gramload (gram)		
		FEA Result	Experiment data	%Difference
Head 0	Outer arm	2.88	2.59	11%
Head 1	Inner arm	2.81	2.63	7%
Head 2	Inner arm	2.38	2.46	3%
Head 3	Outer arm	2.34	2.45	5%

5. Results and Discussions

Finite element simulations of the ball swaging process were performed to study the behaviors and the characteristics of the baseplate after the swaging process. The effects of changing the base plate and arm tip deformation to tip height and tip pitch deviation from nominal value which affect HSA gram load is also investigated. For all simulation cases, the computational results values are in good agreement with averaged test data. Based on the result of this work, an offset could be diminished by improving the precision of swage key shape and swage boss profile .The effects of the ball swaging process on the resulting retention torque of HGA will be evaluated in a future simulation.

6. Acknowledgment

This study is supported by Cooperate Project between National Electronics and Computer Technology Center (NECTEC) and Seagate Technology (Thailand) via Industry/University Cooperative Research Center (I/UCRC) in HDD Component, Khon Kaen University.

7. References

Drean M.; Habraken A.M.; Muzeau J.P.; Bouchair A. (1998), Modelling of the Swaging Process during the Installation of Swaged Bolts, Journal of Constructional Steel Research, Volume 46, Number 1, April 1998, pp. 256-257(2)

Jian Yang, Chen-Chi Lin, Shahab Tabrizi (2007), Finite Element Simulation of Ball Swaging Process of Jointing HGA With Actuator Arm and Gram Load Calculation, ASME Information Storage and Processing Systems Conference, Santa Clara, CA.

Jongpradist, P., Rotbunsongsri, R., Sukkana, C., Sungtong, W (2009), Parametric Study of Baseplate Geometry Using Finite Element Analysis, DST-CON , Bangkok, Thailand

J.R. Cho, J.I. Song, K.T. Noh and D.H. Jeon (2005), Nonlinear finite element analysis of swaging process for automobile power steering hose, Journal of Materials Processing Technology, Volume 170, Issues 1-2 , 14 December 14, Pages 50-57

K. Aoki and K. Aruga(2007), Numerical Ball Swaging Analysis of Head Arm for Hard Disk Drives," Microsyst. Technol., vol. 13, pp. 943-949.

Li RONG, Zuo-ren NIE and Tie-yong ZUO(2006), FEA modeling of effect of axial feeding velocity on strain field of rotary swaging process of pure magnesium, Transactions of Nonferrous Metals Society of China, Volume 16, Issue 5, October 2006, Pages 1015-1020

S. K. Wadhwa(1996), Material Compatibility and Some Understanding of the Ball Swaging Process, IEEE Trans. Magn., vol. 32, no. 3, pp. 1837-1842.

T. Kamnerdtong, S. Chutima and K. Ekintumas (2005), Effects of Swaging Process Parameters on Specimen Deformation, Eighth Asian Symposium on Visualization, Chiangmai, Thailand, pp.50.1-50.7

Zhi-Hua Zhong(1993), Finite element procedures for contact-impact problems, Oxford science publication, Oxford